

LETTER

Open Access



# Self-propagating reactive Al/Ni nanocomposites for bonding applications

Matthias P. Kremer<sup>1,2\*</sup>, Ali Roshanghias<sup>1†</sup> and Andreas Tortschanoff<sup>1†</sup>

## Abstract

Highly reactive integrated material systems have recently gained attention, as they promise a feasible tool for heterogeneous integration of micro electromechanical systems. As integrated energy sources they can be used to join heterogeneous materials without applying too much thermal stress to the whole device. An alternative approach is proposed, comprising a single layer of a reactive nanocomposite made of intermixed metal nanoparticles, instead of multilayer systems. In this study the development of the reactive nanocomposite from choice of materials through processing steps, handling and application methods are described. Eventually the results of the experiments upon the reactivity of the nanocomposites and the feasibility for bonding applications are presented. Analysis of the composites was performed by phase-analysis using x-ray diffraction and reaction propagation analysis by high-speed imaging. Composition of products was found to vary with initial particle sizes. Beside of other phases, the dominant phase was intermetallic NiAl.

**Keywords:** SHS, Reactive nanocomposites, Bonding

## Background

Exothermic reactions have been used as a source of energy for welding and soldering application for well over 100 years [1, 2]. This method, firstly named thermite welding after the reactive mixture Al and iron oxide (thermite), was mainly used in rail track building. The concept uses a self-sustaining exothermic chemical redox reaction at the joint. The reaction products are elementary iron and Al oxide. Due to the high reaction temperatures the iron melts and fills in the joining gap in molten form. In the past 15 years, research groups started to adapt comparable processes for microsystems technologies, using the term of *integrated reactive material systems* [3, 4]. While the new processes completely differ from thermite welding in means of used materials, the concept of using the energy emitted by a self-sustaining reaction for bonding is comparable.

The concepts mostly rely on the following structure: a reactive material composition is applied to the gap in between the two surfaces which are to be joined. The bonding surfaces are coated with a solder layer. While applying pressure, the intermediate reactive layer is ignited by a short pulse of energy (e.g. electric current, heat contact, laser pulse) and the following exothermic reaction leads to melting of the solder. The solder solidifies immediately after the reaction front has passed and forms a bond at the adjacent surfaces. As the process takes place in only a few milliseconds and the emitted energy is mainly used for melting the solder, the surrounding material's temperature does not significantly rise [5].

Common among the new processes is the usage of reactive multilayer systems. These systems comprise layers with a thickness in the nanometer regime and are alternately stacked up to a total thickness of some tens of micrometers [5]. Main advantage of multilayer systems is the large reactive surface area leading to very high reaction front propagation velocities in the regime of tens of meters per second. The inherent disadvantages of multilayer systems are the time consuming, complex and expensive manufacturing of many alternating layers and the need for patterning of the reactive system [6].

\*Correspondence: matthias.kremer@partner.kit.edu

†Ali Roshanghias and Andreas Tortschanoff contributed equally to this work

<sup>2</sup> Institute of Microstructure Technology, Karlsruhe Institute of Technology, Hermann-von-Helmholtz-Platz 1, Eggenstein-Leopoldshafen, Germany  
Full list of author information is available at the end of the article

Overcoming these problems, the concept of a bonding process based on a single layer reactive nanocomposite (RNC) which can be deposited in arbitrary patterns was developed [7]. Figure 1 shows a drawing of the bonding concept using RNC with only four process steps. Step one is to deposit the reactive nanocomposite dispersed into a carrier fluid onto the bottom substrate in an arbitrary pattern. After the carrier fluid is removed by evaporation, in step two, the top substrate is aligned. Step three is to ignite the RNC layer while applying pressure to the substrates. After the reaction has passed, the bond is finished (step four) and the surrounding areas were not heated significantly.

### Materials and processing

An extensive overview of material combinations which can undergo the desired kind of reaction is given by Adams in an excellent review on the applications of reactive multilayer systems [8], which to study the reader is

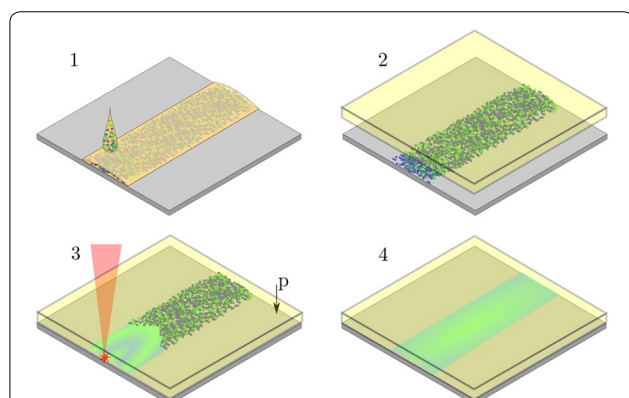


**Fig. 1** Drawing of the concept of reactive nanocomposites (RNC) based bonding. 1 Deposition of the nanocomposite mixture dispersed in a carrier fluid onto the bottom substrate. 2 Removal of carrier fluid by evaporation and alignment of top substrate. 3 Ignition of the reactive bonding layer by a laser pulse through the top substrate while applying pressure. 4 Finished bond. The surrounding areas are not heated significantly

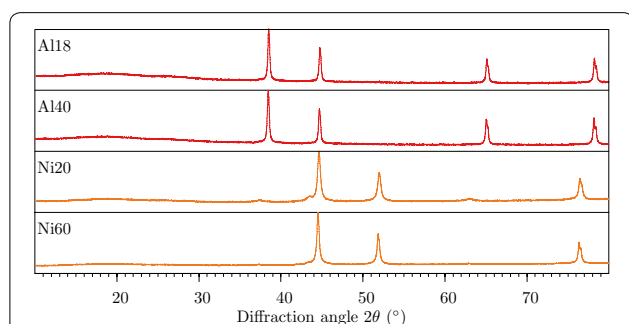


**Fig. 2** XRD graph of the initial nanoparticles batches. All samples show high material purity with negligible oxygen contamination

strongly encouraged. Although various material combinations are capable of executing self-propagating high temperature reactions, according to Adams, the majority of research is attributed to the Ni/Al system.

Table 1 shows the key properties of the material combination that was evaluated for the RNC development. Important properties are the specific reaction enthalpy and the adiabatic reaction temperature. The Ni/Al system shows sufficiently high values for both properties in comparison to other possible materials combinations, such as Al+Ti or Ti+Ni [9]. As initial experimental results were most promising with the Ni/Al system, further investigations were concentrated on this system.

Pure elemental Ni- and Al-nanoparticles were acquired from Iolitec (Heilbronn, Germany). Four sample batches were used with particles of spherical shape with equiatomic mixtures of Ni and Al particles. Table 2 gives an overview of the particle sizes as declared and as measured and the nomenclature which is used in this article for the batches. Accordingly to the raw materials nomenclature, the sample mixtures were named *Al18Ni20*, *Al18Ni60*, *Al40Ni20*, *Al40Ni60*.

Chemical composition of the educt batches was evaluated by XRD measurement, showing no oxide phase formation to the detection level of XRD, as shown in Fig. 2. All processing and experimental steps were conducted in a glove box with clean inert (99.99990% argon) atmosphere to prevent passivation of the reactive materials and any other unintended reactions.

### Experiments and results

Wet and dry mixing of metallic nanoparticles were compared. The prior was executed using cyclohexane as a solvent for dispersing the nanoparticles. The latter was

**Table 1 Properties of the materials combination used for the RNC development [13]**

Reaction mechanism	Ni+Al → NiAl
Reaction enthalpy $\Delta H_f$	-59 kJ/mol
Adiabatic reaction temperature $T_{Ad}$	1900 K
Reference	[13]

**Table 2 Batch description and particle sizes of the acquired material**

Batch name	Material	Specified diameter (nm)	Measured diameter (nm)
Al18	Aluminium	18	41 ± 21
Al40	Aluminium	40–60	80 <sup>a</sup>
Ni20	Nickel	20	47 ± 18
Ni60	Nickel	60–80	100 <sup>a</sup>

<sup>a</sup> Estimated particle size of these batches based on SEM graphs

executed using manual grinding of the nanoparticles in a porcelain mortar. The procedure for wet mixing was as follows: nanoparticles of Al and Ni were dispersed in equi-atomic ratio in cyclohexane. The particles were of spherical shape and the particles' diameters were 18 or 40 nm for the Al and 20 and 60 nm for the Ni particles. Sample batches were named by composition of material and particle size, e.g. Al18Ni20 for a mixture of Al particles with 18 nm and Ni particles with 20 nm diameter, respectively.

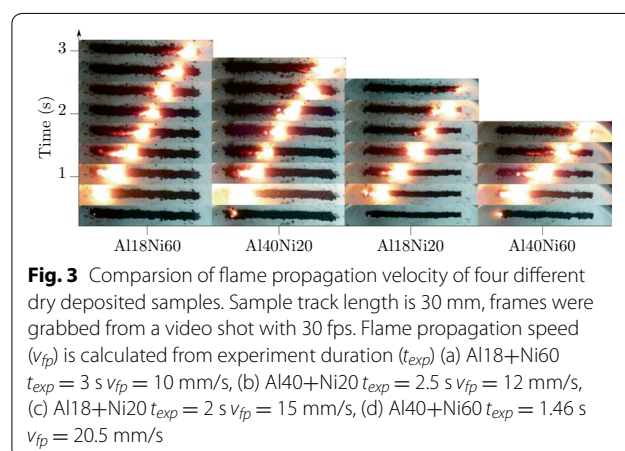
After dispersing the particles into the solvent, ultrasonic agitation was applied at 48 kHz and approximately 20 W. After ultrasonification the dispersion was dispensed onto sample substrates, made from silicon and copper. After dispensing, the solvent was evaporated at room temperature or elevated temperature. All experiments were conducted under inert Ar atmosphere. After evaporation of the solvent the residual particles form the reactive layer. Ignition of the reactive layer was executed using laser radiation. A laser diode with a wavelength of  $\lambda = 808$  nm and optical power  $p = 166$  mW was used. Variations of all parameters like particle size, particle size ratio, atomic ratio, ultrasonification time, dispersion concentration, ignition temperature, laser power, substrate material, materials combination were performed, each experiment leading to the same result that dispersed Al-Ni mixtures were not ignitable. XRD (x-ray powder diffraction) and EDX (energy dispersive x-ray spectroscopy) analysis showed significant oxygen contamination on all samples. This leads to the conclusion, that reactions were constrained by passivation layers on the particles. XRD spectra of wet and dry deposited samples are compared in the Additional file 1.

Mechanical activation with high energy ball milling was reported to enhance reactivity of reactive nanomaterials [10]. In contrast to the wet mixed composites, ignition experiments with mechanically activated samples were successful. Other than in the literature, mechanical activation was not conducted using a mill, but by simple manual pestling of the particles in a porcelain mortar for several minutes. RNC sample batches of equiatomic Al18Ni20, Al18Ni60, Al40Ni20 and Al40Ni60 particles were weighted into the mortar. After pestling, the particles were removed from the mortar for further processing. Two sets of experiments were conducted. In the first set, the particles were dry deposited onto the substrate. In the second step the particles were dispersed in cyclohexane for dispensing and after deposition dried in a vacuum chamber. Ignition tests were performed using the same laser setup as aforementioned. Self-propagating high temperature reactions were observed in the RNC layer with a maximum reaction front propagation velocity of 20.5 mm/s. Figure 3 shows sequences of captured

images from videos taken of reactivity experiments of different material compositions on a time scale. The reaction front propagation velocity varies by a factor of two, depending on the particle combination.

XRD analysis of the grinded samples showed spectra matching the combined spectra of the respective pure Al and Ni particles, showing that no phase transformation takes place during mixing and grinding, hence the process of mechanical activation does not involve mechanical alloying.

Reactivity is quantified by measuring the reaction front propagation velocity and the amount of unreacted material in the sample after the reaction. Particle size and the difference in density of Al and Ni lead to large differences in the ratio of number of particles per material. As all samples were prepared with the same stoichiometry (1:1), the chemical composition is constant and not expected to influence the reactivities. Reactivity of the sample was found to correlate with the number of particles per material ratio. Figure 4 shows the reaction front propagation velocity and the amount of reacted material over the number of particles ratio. Both parameters show a peak in the region of 1–10 Al particles per Ni particle. The highest velocity and reacted fraction were measured at the Al40Ni60 sample, followed shortly after by the Al18Ni20 sample. Both, velocity and reacted fraction were much lower for the other two samples, Al18Ni60 and Al40Ni20. Figure 5 shows XRD graphs of the reaction products and mass fraction distribution of different phases in the products. Besides some unreacted material, up to four different phases were found in the products, namely  $\text{Ni}_2\text{Al}_3$ , NiAl,  $\text{Ni}_3\text{Al}$  (cubic) and  $\text{Ni}_3\text{Al-T}$  (tetragonal). Mixed to a 1:1 stoichiometry, the intermetallic NiAl phase was expected to dominate. Any amounts of other phases or unreacted particles are presumably a result of inhomogeneous material distribution throughout the reactive layer. The Al40Ni60 sample, which showed the smallest amount of unreacted material also reveals the



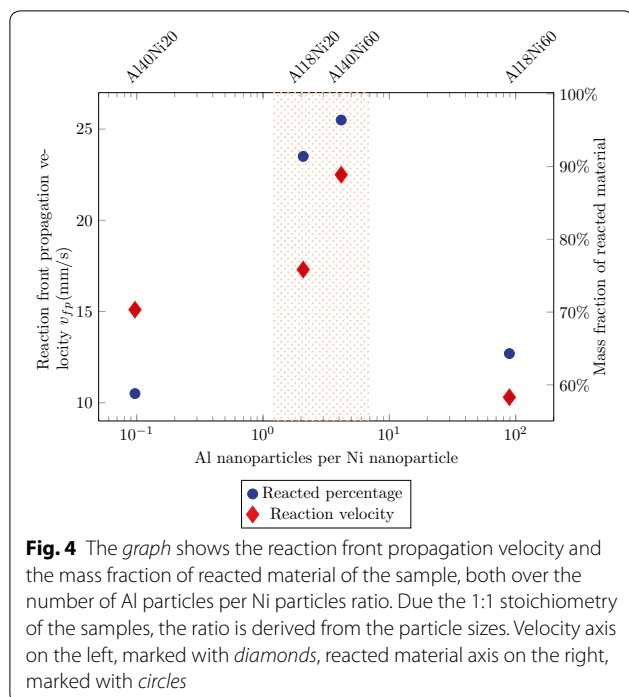


**Fig. 4** The graph shows the reaction front propagation velocity and the mass fraction of reacted material of the sample, both over the number of Al particles per Ni particles ratio. Due the 1:1 stoichiometry of the samples, the ratio is derived from the particle sizes. Velocity axis on the left, marked with diamonds, reacted material axis on the right, marked with circles

largest fraction of the desired NiAl phase. It is worth noting, that no differences were measured in the reactivity between dry and wet deposited samples.

**Conclusion**

Experiments upon the reactivity of four different mixtures of Al and Ni nanoparticles were conducted. All mixtures were prepared in an equiatomic ratio (stoichiometry 1:1) with only the particle sizes varying.

The nanoparticles were of spherical shape with diameters in the range of 18 to 80 nm. Self-propagating high temperature synthesis reactions were initiated by laser ignition of mechanically activated samples.

Mechanical activation was conducted by pestling the particles in a ceramic mortar. Reactivity of a sample was quantified by measuring the reaction front propagation velocity using high speed imaging and the amount of reacted material using XRD analysis of the reaction product.

It was found that reactivity of the samples greatly differs depending on the ratio of Al particles per Ni particle. The Al40Ni60 sample showed the highest reaction front propagation velocity (20.5 mm/s). Two possible reasons for the increased reactivity of this sample are presented:

1. As all samples were prepared with a 1:1 stoichiometry the size proportion of this sample’s particles leads to an approximate equal number of particles per

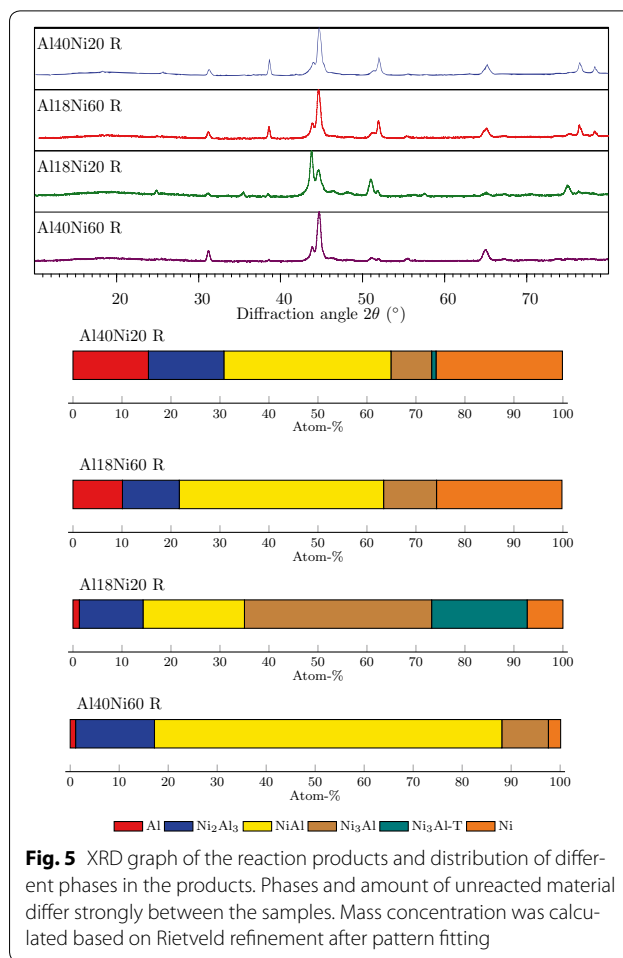


**Fig. 5** XRD graph of the reaction products and distribution of different phases in the products. Phases and amount of unreacted material differ strongly between the samples. Mass concentration was calculated based on Rietveld refinement after pattern fitting

material. Thus leading to a homogeneous distribution of “reaction points”, which is the contact of two particles with differing materials, throughout the sample and an approximate equal number of reaction points per reactive particle.

2. As the diameters are the largest, an occasional passivation layer (like oxygen contamination, i.e.) would have the smallest influence on the total amount of reactive material. Passivation layers’ thicknesses tend to be not depending on the particle diameter, hence a passivation layer with about 4 nm thickness would lead to about 53% passivated material for 18nm particles but only 19% passivated material for 60 nm particles, respectively. Although the reacted materials did not show significant oxygen contamination this generally has to be considered critical when dealing with ultra-small reactive particles. In other studies, extensive efforts were driven to lower the reaction velocity, achieving values in the same order of magnitude as this work [11]. The highest amount of reacted material was also measured for the Al40Ni60 sam-

ple with (96.4%). In these experiments the samples were deposited onto a bottom substrate, but no top substrate was pressed on top of it. It was found that application of a top substrate lead to a high probability for quenching of the reactions. A reaction front passing through the whole sample without reaction quenching is essential to establish bonding. Heat transfer of the reaction into the substrates has to be carefully considered—it is necessary to have a sufficient amount of heat transferred into the solder layer to enable melting, while at the same time provide enough energy to keep the reaction self-sustaining. To enable reactive bonding with a RNC layer high reactivity is desirable to prevent reaction quenching by heat transfer into the substrates.

Therefore, in further studies, focus shall be set on the Al40Ni60 system. Comparing the reactivity of the commercial reactive bonding tool *NanoFoil* (2–10 m/s) with our Al40Ni60 RNC system by the reaction front propagation velocity shows a reactivity about 2–3 orders of magnitude larger for the *NanoFoil* [12]. High energy ball milling shall be employed in following studies instead of manual pestling to increase the reactivity of the RNC layer. In addition, the rheological properties of the RNC dispersion shall be investigated to enable ink-jet printing of the RNC layer instead of dispensing.

Though not yet realized, using dispensable reactive nanocomposites as heat source for bonding applications in microsystems technologies seems a very promising concept which is well worth further investigations.

### Additional file

**Additional file 1: Figure S1.** XRD graphs of the grinded samples, showing only Al and Ni phases. **Figure S2.** Representative SEM image of an Al40Ni60 sample. **Figure S3.** Comparison of XRD measurements of grinded and sonicated Al18Ni20 samples. The sonicated sample shows vast amounts of Al2O3, while the grinded sample shows no oxidized phases.

### Authors' contributions

MPK developed the RNC concept and executed all experimental work. AR and AT contributed to data analysis and process development. All authors read and approved the final manuscript.

### Author details

<sup>1</sup> CTR Carinthian Tech Research AG, Europastr. 12, Villach, Austria. <sup>2</sup> Institute of Microstructure Technology, Karlsruhe Institute of Technology, Hermann-von-Helmholtz-Platz 1, Eggenstein-Leopoldshafen, Germany.

### Acknowledgements

Academic supervision by and fruitful discussion with Prof. Andreas E. Guber is greatly acknowledged. The authors want to thank Ernst Hinteregger from Treibacher Industrie AG for support with SEM, EDX and XRD analysis.

### Competing interests

The authors declare that they have no competing interests.

### Funding

The project EPPL is co-funded by Grants from Austria, Germany, The Netherlands, France, Italy, Portugal and the ENIAC Joint Undertaking and is coordinated by Infineon Technologies Austria AG.

Received: 14 October 2016 Accepted: 27 January 2017

Published online: 08 February 2017

### References

1. Goldschmidt H, Vautin C (1898) Aluminium as a heating and reducing agent. *J Soc Chem Ind* 17(6):543–545. doi:10.1002/jctb.5000170601
2. Dong S, Hou P, Yang H, Zou G (2002) Synthesis of intermetallic NiAl by SHS reaction using coarse-grained nickel and ultrafine-grained aluminum produced by wire electrical explosion. *Intermetallics* 10(3):217–223. doi:10.1016/S0966-9795(01)00109-1
3. Braeuer J, Besser J, Wiemer M, Gessner T (2012) A novel technique for MEMS packaging: reactive bonding with integrated material systems. *Sens Actuators A Phys* 188:212–219. doi:10.1016/j.sna.2012.01.015
4. Weihs TP, Reiss M (2001) Method of making reactive multilayer foil and resulting product. European Patent Number EP 1278 631 B1
5. Weihs TP (2014) Fabrication and characterization of reactive multilayer films and foils. In: Katayun Barmak KC (ed) *Metallic films for electronic, optical and magnetic applications*, vol 1. Elsevier, Cambridge, pp 160–243. doi:10.1533/9780857096296.1.160
6. Braeuer J, Besser J, Hertel S, Masser R, Schneider W, Wiemer M, Gessner T (2014) (Invited) Reactive bonding with integrated reactive and nano scale energetic material systems (iRMS): State-of-the-Art and Future Development Trends. *ECS Trans* 64(5):329–337. doi:10.1149/06405.0329ecst
7. Kremer MP, Tortschanoff A, Guber AE (2015) Reactive nanocomposites for heterogeneous integration. In: Gessner T (ed) *Smart Systems Integration 2015*, vol 1. Apprimus Verlag, Aachen, pp 418–421. ISBN:978-3-86359-296-7
8. Adams DP (2015) Reactive multilayers fabricated by vapor deposition: a critical review. *Thin Solid Films* 576:98–128. doi:10.1016/j.tsf.2014.09.042
9. Dietrich G, Braun S, Gawlitza P, Leson A (2009) Reaktive Nanometer-Multischichten als maßgeschneiderte Wärmequellen beim Fügen. *Vakuum in Forschung und Praxis* 21(1):15–21. doi:10.1002/vipr.200900375
10. Mukasyan AS, Rogachev AS, Aruna ST (2015) Combustion synthesis in nanostructured reactive systems. *Adv Powder Technol* 26(3):954–976. doi:10.1016/j.apt.2015.03.013
11. Fritz GM, Jores H, Weihs TP (2011) Enabling and controlling slow reaction velocities in low-density compacts of multilayer reactive particles. *Combust Flame* 158(6):1084–1088. doi:10.1016/j.combustflame.2010.10.008
12. Indium: NanoFoil properties. <http://www.indium.com/nanofoil/properties/>. Accessed 27 Nov 2016
13. Weihs TP, Knio O, Reiss M, Blobaum KJ (2001) Reactive Multilayer Structures for ease of processing and enhanced ductility. US Patent Number US20010046597